

HIGGS BOSON PRODUCTION AT HADRON COLLIDERS: SIGNAL AND BACKGROUND PROCESSES

David Rainwater¹, Michael Spira² and Dieter Zeppenfeld³

¹ *Fermilab, Batavia, IL, 60510, USA*

² *Paul Scherrer Institut, CH-5232 Villigen PSI, Switzerland*

³ *Department of Physics, University of Wisconsin, Madison, WI 53706, USA*

Abstract

We review the theoretical status of signal and background calculations for Higgs boson production at hadron colliders. Particular emphasis is given to missing NLO results, which will play a crucial role for the Tevatron and the LHC.

1 Introduction

The Higgs mechanism is a cornerstone of the Standard Model (SM) and its supersymmetric extensions. Thus, the search for Higgs bosons is one of the most important endeavors at future high-energy experiments. In the SM one Higgs doublet has to be introduced in order to break the electroweak symmetry, leading to the existence of one elementary Higgs boson, H [1]. The scalar sector of the SM is uniquely fixed by the vacuum expectation value v of the Higgs doublet and the mass m_H of the physical Higgs boson [2]. The negative direct search for the Higgsstrahlung process $e^+e^- \rightarrow ZH$ at the LEP2 collider poses a lower bound of 114.1 GeV on the SM Higgs mass [3], while triviality arguments force the Higgs mass to be smaller than ~ 1 TeV [4].

Since the minimal supersymmetric extension of the Standard Model (MSSM) requires the introduction of two Higgs doublets in order to preserve supersymmetry, there are five elementary Higgs particles, two CP-even (h, H), one CP-odd (A) and two charged ones (H^\pm). At lowest order all couplings and masses of the MSSM Higgs sector are fixed by two independent input parameters, which are generally chosen as $\tan\beta = v_2/v_1$, the ratio of the two vacuum expectation values $v_{1,2}$, and the pseudoscalar Higgs-boson mass m_A . At LO the light scalar Higgs mass m_h has to be smaller than the Z -boson mass m_Z . Including the one-loop and dominant two-loop corrections the upper bound is increased to $m_h \lesssim 135$ GeV [5]. The negative direct searches for the Higgsstrahlung processes $e^+e^- \rightarrow Zh, ZH$ and the associated production $e^+e^- \rightarrow Ah, AH$ yield lower bounds of $m_{h,H} > 91.0$ GeV and $m_A > 91.9$ GeV. The range $0.5 < \tan\beta < 2.4$ in the MSSM is excluded by the Higgs searches at the LEP2 experiments [3].

The intermediate mass range, $m_H < 196$ GeV at 95% CL, is also favored by a SM analysis of electroweak precision data [3]. In this contribution we will therefore concentrate on searches and measurements for $m_H \lesssim 200$ GeV. The Tevatron has a good chance to find evidence for such a Higgs boson, provided that sufficient integrated luminosity can be accumulated [6]. The Higgs boson, if it exists, can certainly be seen at the LHC, and the LHC can provide measurements of the Higgs boson mass at the 10^{-3} level [7], and

measurements of Higgs boson couplings at the 5 to 10% level [8]. Both tasks, discovery and measurement of Higgs properties, require accurate theoretical predictions of cross sections at the LHC, but these requirements become particularly demanding for accurate coupling measurements.

In this contribution we review the present status of QCD calculations of signal and background cross sections encountered in Higgs physics at hadron colliders. Desired accuracy levels can be estimated by comparing to the statistical errors in the determination of signal cross sections at the LHC. For processes like $H \rightarrow \gamma\gamma$, where a very narrow mass peak will be observed, backgrounds can be accurately determined directly from data. For other decay channels, like $H \rightarrow b\bar{b}$ or $H \rightarrow \tau\tau$, mass resolutions of order 10% require modest interpolation from sidebands, for which reliable QCD calculations are needed. Most demanding are channels like $H \rightarrow W^+W^- \rightarrow l^+l^-p_T$, for which broad transverse mass peaks reduce Higgs observation to, essentially, a counting experiment. Consequently, requirements on theory predictions vary significantly between channels. In the following we discuss production and decay channels in turn and focus on theory requirements for the prediction of signal and background cross sections. Because our main interest is in coupling measurements, we will not consider diffractive channels in the following, which are model-dependent and have large rate uncertainties [9]. Potentially, they might contribute to Higgs discovery if, indeed, cross sections are sufficiently large.

2 Gluon fusion

The gluon fusion mechanism $gg \rightarrow \phi$ provides the dominant production mechanism of Higgs bosons at the LHC in the entire relevant mass range up to about 1 TeV in the SM and for small and moderate values of $\tan\beta$ in the MSSM [10]. At the Tevatron this process plays the relevant role for Higgs masses between about 130 GeV and about 190 GeV [6]. The gluon fusion process is mediated by heavy quark triangle loops and, in the case of supersymmetric theories, by squark loops in addition, if the squark masses are smaller than about 400 GeV [11], see Fig. 1.

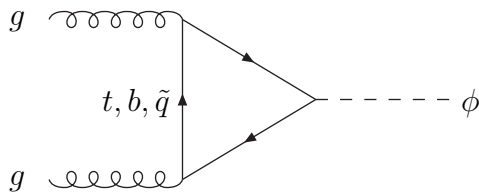


Figure 1: *Typical diagram contributing to $gg \rightarrow \phi$ at lowest order.*

In the past the full two-loop QCD corrections have been determined. They increase the production cross sections by 10–80% [12], thus leading to a significant change of the theoretical predictions. Very recently, Harlander and Kilgore have finished the full NNLO calculation, in the heavy top quark limit [13, 14]. This limit has been demonstrated to

approximate the full massive K factor at NLO within 10% for the SM Higgs boson in the entire mass range up to 1 TeV [15]. Thus, a similar situation can be expected at NNLO. The reason for the quality of this approximation is that the QCD corrections to the gluon fusion mechanism are dominated by soft gluon effects, which do not resolve the one-loop Higgs coupling to gluons. Fig. 2 shows the resulting K -factors at the LHC and the scale variation of the K -factor. The calculation stabilizes at NNLO, with remaining scale variations at the 10 to 15% level. These uncertainties are comparable to the experimental errors which can be achieved with 200 fb^{-1} of data at the LHC, see solid lines in Fig. 3. The full NNLO results confirm earlier estimates which were obtained in the frame work of soft gluon resummation [15] and soft approximations [16] of the full three-loop result. The full soft gluon resummation has been performed in Ref. [17]. The resummation effects enhance the NNLO result by about 10% thus signaling a perturbative stabilization of the theoretical prediction for the gluon-fusion cross section.

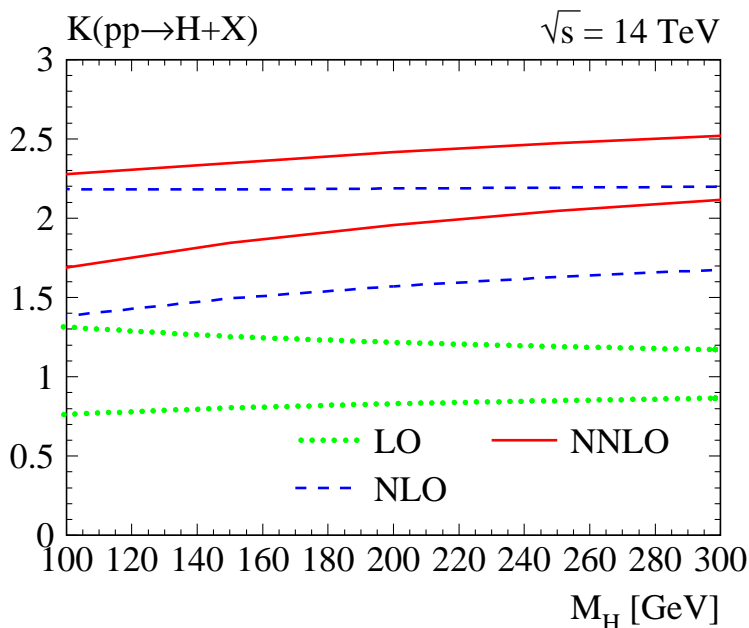


Figure 2: Scale dependence of the K -factor at the LHC. Lower curves for each pair are for $\mu_R = 2m_H$, $\mu_F = m_H/2$, upper curves are for $\mu_R = m_H/2$, $\mu_F = 2m_H$. The K -factor is computed with respect to the LO cross section at $\mu_R = \mu_F = m_H$. From Ref. [14].

In supersymmetric theories the gluon fusion cross sections for the heavy Higgs, H , and, for small m_A , also for the light Higgs, h , may be dominated by bottom quark loops for large values of $\tan\beta \gtrsim 10$ so that the heavy top quark limit is not applicable. This can be clearly seen in the NLO results, which show a decrease of the K factor down to about 1.1 for large $\tan\beta$ [12]. This decrease originates from an interplay between the large positive soft gluon effects and large negative double logarithms of the ratio between the Higgs and bottom masses. In addition, the shape of the p_T distribution of the Higgs boson may be altered; if the bottom loop is dominant, the p_T spectrum becomes softer than in the case of top-loop dominance. These effects lead to some model dependence of predicted cross sections.

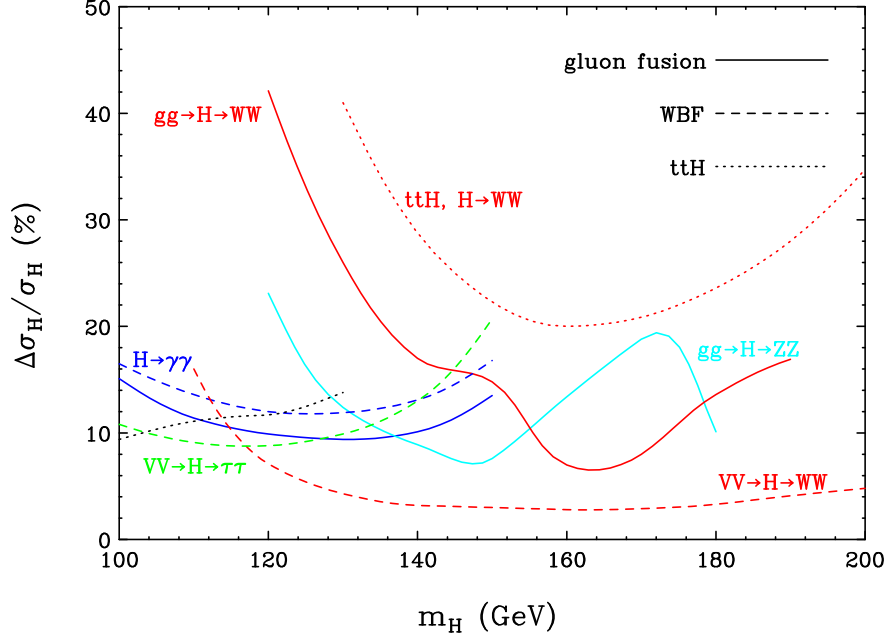


Figure 3: *Expected relative error on the determination of $B\sigma$ for various Higgs search channels at the LHC with 200 fb^{-1} of data [8]. Solid lines are for inclusive Higgs production channels which are dominated by gluon fusion. Expectations for weak boson fusion are given by the dashed lines. Dotted lines are for $t\bar{t}H$ production with $H \rightarrow b\bar{b}$ [18] (black) and $H \rightarrow W^+W^-$ [44] (red). The latter assumes 300 fb^{-1} of data.*

Let us now turn to a discussion of backgrounds for individual decay modes.

(i) $\phi \rightarrow \gamma\gamma$

At the LHC the SM Higgs boson can be found in the mass range up to about 150 GeV by means of the rare photonic decay mode $H \rightarrow \gamma\gamma$ [7]. The dominant Higgs decays $H \rightarrow b\bar{b}, \tau^+\tau^-$ are overwhelmed by large QCD backgrounds in inclusive searches. The QCD $\gamma\gamma$ background is known at NLO, including all relevant fragmentation effects. The present status is contained in the program DIPHOX [19]. The loop mediated process $gg \rightarrow \gamma\gamma$ contributes about 50% to the $\gamma\gamma$ background and has been calculated at NLO very recently [20]. However, a numerical analysis of the two-loop result is still missing.

Once the experiment is performed, the diphoton background can be determined precisely from the data, by a measurement of $d\sigma/dm_{\gamma\gamma}$ on both sides of the resonance peak. The NLO calculations are useful, nevertheless, for an accurate prediction of expected accuracies and for a quantitative understanding of detector performance.

(ii) $H \rightarrow W^+W^-$

This mode is very important for Higgs masses above W -pair but below Z -pair threshold, where $B(H \rightarrow WW)$ is close to 100%. In order to suppress the $t\bar{t} \rightarrow b\bar{b}W^+W^-$ background for W^+W^- final states, a jet veto is crucial. However, gluon fusion receives sizeable contributions from real gluon bremsstrahlung at NLO, which will also be affected by the jet veto. These effects have recently been analyzed in Ref. [21], in the soft approximation to the full NNLO calculation. A veto of additional jets with $p_{Tj} > 15 \text{ GeV}$, as e.g.

envisioned by ATLAS [7], reduces the NNLO K -factor to about $K = 0.8^*$, i.e. one loses more than 60% of signal events. In addition the scale dependence of the cross section starts to grow with such stringent veto criteria. These effects need to be modeled with a NLO Monte Carlo program for $H + jet$ production in order to reach a reliable quantitative result for the signal rate. Since stop and sbottom loops are sizeable in supersymmetric theories for squark masses below about 400 GeV, their inclusion is important in these investigations.

From the perspective of background calculations, $H \rightarrow WW$ is the most challenging channel. Backgrounds are of the order of the signal rate or larger, which requires a 5% determination or better for the dominant background cross sections in order to match the statistical power of LHC experiments. In fact, the large errors at $m_H \lesssim 150$ GeV depicted in Fig. 3 ($gg \rightarrow H \rightarrow WW$ curve) are dominated by an assumed 5% background uncertainty. Clearly, such small errors cannot be achieved by NLO calculations alone, but require input from LHC data. Because of two missing neutrinos in the $W^+W^- \rightarrow l^+l^- \cancel{p}_T$ final state, the Higgs mass cannot be reconstructed directly. Rather, only wide ($l^+l^-; \cancel{p}_T$) transverse mass distributions can be measured, which do not permit straightforward side-band measurements of the backgrounds. Instead one needs to measure the normalization of the backgrounds in signal poor regions and then extrapolate these, with the help of differential cross sections predicted in perturbative QCD, to the signal region. The theory problem is the uncertainty in the shape of the distributions used for the extrapolation, which will depend on an appropriate choice of the “signal poor region”. No analysis of the concomitant uncertainties, at LO or NLO QCD, is available to date.

After the jet veto discussed above, the dominant background processes are $pp \rightarrow W^+W^-$ and (off-shell) $t\bar{t}$ production [7]. W^+W^- production is known at NLO [22] and available in terms of parton level Monte Carlo programs. In addition, a full NLO calculation including spin correlations of the leptonic W, Z decays, in the narrow width approximation, is available [23]. For Higgs boson masses below the $W^+W^-(ZZ)$ threshold, decays into $WW^*(ZZ^*)$ are important [24, 10]. Since hadron colliders will be sensitive to these off-shell tails, too, the backgrounds from VV^* production become relevant. There is no NLO calculation of VV^* background processes available so far, so that it is not clear if NLO effects will be significant in the tails of distributions needed for the Higgs search in these cases. Moreover, for WW^* production the inclusion of spin correlations among the final state leptons is mandatory [25].

Top quark backgrounds arise from top-pair and tWb production. Recently, a new theoretical analysis of $pp \rightarrow t^{(*)}\bar{t}^{(*)}$ has become available including full lepton correlations and off-shell effects of the final state top quarks arising from the non-zero top decay width [26]. This calculation automatically includes $pp \rightarrow tbW$ and those contributions to $pp \rightarrow b\bar{b}W^+W^-$, which are gauge-related to tbW couplings and describes the relevant tails for the Higgs search at LO. It is now necessary to investigate the theoretical uncertainties of this background. A NLO calculation of off-shell top-pair production may well be needed to reach the required 5% accuracy for extrapolation to the Higgs search region.

Other important reducible backgrounds are the $Wt\bar{t}$, $Zt\bar{t}$, $Wb\bar{b}$ and $Zb\bar{b}$ production processes. While $Vt\bar{t}$ ($V = W, Z$) production is only known at LO, the associated vector

* It should be noted that for this strong cut in $p_{T,j}$ the NNLO result may be plagued by large logarithms of this cut, which have to be resummed, see [17].

boson production with $b\bar{b}$ pairs is known at NLO including a soft gluon resummation [27]. Thus $Vb\bar{b}$ production can be considered as reliable from the theoretical point of view, while a full NLO calculation for $Vt\bar{t}$ production is highly desirable, since top mass effects will play a significant role. In addition, the background from $gb \rightarrow tH^-$, $g\bar{b} \rightarrow \bar{t}H^+$ has to be taken into account within the MSSM framework. The full LO matrix elements are included in the ISAJET Monte Carlo program, which can easily be used for experimental analyses.

(iii) $H \rightarrow ZZ \rightarrow 4\ell^\pm$

A sharp Higgs peak can be observed in the four lepton invariant mass distribution. Hence, the $ZZ \rightarrow 4\ell^\pm$ backgrounds are directly measurable in the sidebands and can safely be interpolated to the signal region.

3 $qq \rightarrow qqH$

In the SM the WW, ZZ fusion processes $qq \rightarrow qqV^*V^* \rightarrow qqH$ play a significant role at the LHC for the entire Higgs mass range up to 1 TeV. We refer to them as weak boson fusion (WBF). The WBF cross section becomes comparable to the gluon fusion cross section for Higgs masses beyond ~ 600 GeV [10] and is sizable, of order 20% of $\sigma(gg \rightarrow H)$, also in the intermediate mass region. The energetic quark jets in the forward and backward directions allow for additional cuts to suppress the background processes to WBF. The NLO QCD corrections can be expressed in terms of the conventional corrections to the DIS structure functions, since there is no color exchange between the two quark lines at LO and NLO. NLO corrections increase the production cross section by about 10% and are thus small and under theoretical control [28, 29]. These small theory uncertainties make WBF a very promising tool for precise coupling measurements. However, additional studies are needed to assess the theoretical uncertainties associated with a central jet veto. This veto enhances the color singlet exchange of the signal over color octet exchange QCD backgrounds [30–33].

In the MSSM, first parton level analyses show that it should be possible to cover the full MSSM parameter range by looking for the light Higgs decay $h \rightarrow \tau^+\tau^-$ (for $m_A \gtrsim 150$ GeV) and/or the heavy Higgs $H \rightarrow \tau^+\tau^-$ resonance (for a relatively small m_A) in the vector-boson fusion processes [34]. Although these two production processes are suppressed with respect to the SM cross section, their sum is of SM strength.

For the extraction of Higgs couplings it is important to distinguish between WBF and gluon fusion processes which lead to $H + jj$ final states. With typical WBF cuts, including a central jet veto, gluon fusion contributions are expected at order 10% of the WBF cross section, i.e. the contamination is modest [35, 36]. The gluon fusion processes are mediated by heavy top and bottom quark loops, in analogy to the LO gluon fusion diagram of Fig. 1. The full massive cross section for $H + jj$ production via gluon fusion has been obtained only recently [35], while former analyses were performed in the heavy top quark limit [37]. Since stop and sbottom loops yield a sizeable contribution to the inclusive gluon fusion cross section, a similar feature is expected for $H + jj$ production. Thus, it is important to compute the effects of stop and sbottom loops in $H + jj$ gluon fusion processes, which has not been done so far.

(i) $H \rightarrow \gamma\gamma$

Parton level analyses show that $H \rightarrow \gamma\gamma$ decays in WBF Higgs production can be isolated with signal to background ratios of order one [30] and with statistical errors of about 15%, for 200 fb^{-1} of data (see Fig. 3). Like for the inclusive $H \rightarrow \gamma\gamma$ search, background levels can be precisely determined from a sideband analysis of the data. Prior to data taking, however, full detector simulations are needed to confirm the parton level results and improve on the search strategies.

Improved background calculations are desirable as well. In particular, the $pp \rightarrow \gamma\gamma jj$ background via quark loops (see Fig. 4) has not been calculated so far.

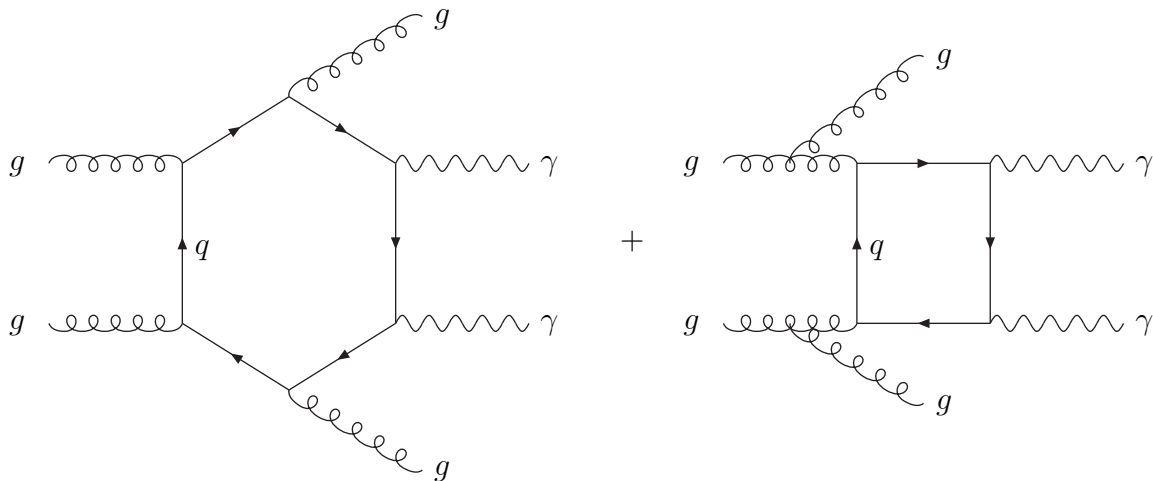


Figure 4: *Typical diagrams contributing to $gg \rightarrow \gamma\gamma jj$ at lowest order.*

(ii) $H \rightarrow \tau^+\tau^-$

The observation of $H \rightarrow \tau\tau$ decays in WBF will provide crucial information on Higgs couplings to fermions [8] and this channel alone guarantees Higgs observation within the MSSM [34] and may be an important discovery channel at low pseudoscalar mass, m_A . Recent detector simulations [36] confirm parton level results [31] for the observability of this channel. (See Fig. 3 for parton level estimates of statistical errors.)

The $\tau^+\tau^-$ -invariant mass can be reconstructed at the LHC with a resolution of order 10%. This is possible in the $qq \rightarrow qqH$ mode because of the large transverse momentum of the Higgs. In turn this means a sideband analysis can be used, in principle, to directly measure backgrounds. The most important of these backgrounds is QCD Zjj production (from QCD corrections to Drell-Yan) or electroweak Zjj production via WBF [31]. The (virtual) Z (or photon) then decays into a $\tau^+\tau^-$ pair. These Zjj backgrounds, with their highly nontrivial shape around $m_{\tau\tau} \approx m_Z$, can be precisely determined by observing $Z \rightarrow e^+e^-, \mu^+\mu^-$ events in identical phase space regions. Theoretically the QCD Zjj background is under control also, after the recent calculation of the full NLO corrections [38]. For the $\tau^+\tau^-$ backgrounds the inclusion of τ polarization effects is important in order to obtain reliable tau-decay distributions which discriminate between signal processes ($h, H \rightarrow \tau^+\tau^-$) and backgrounds. This can be achieved by linking the TAUOLA program [39] to existing Monte Carlo programs.

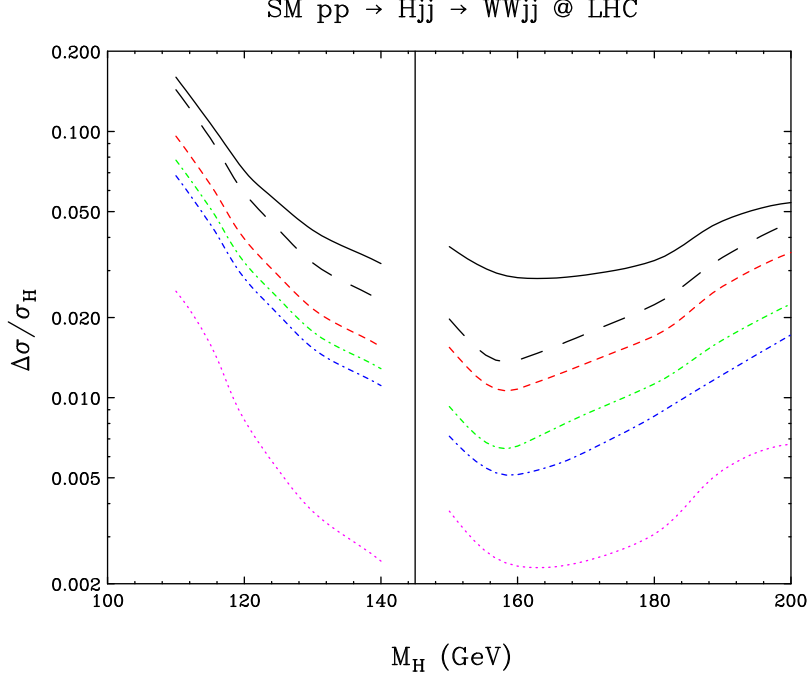


Figure 5: Contributions of background systematic errors $\Delta\sigma$ to a measurement of $\sigma_H = \sigma B(H \rightarrow WW)$ in WBF. Shown, from bottom to top, are the effects of a 10% uncertainty of the $\tau\tau jj$ rate (dotted line), a 50% error on the QCD $WWjj$ rate (blue dash-dotted), a 30% error on the electroweak $WWjj$ rate (green dash-dotted), and a 10% error on $\sigma(tt+jets)$ (red dashes). The long-dashed line adds these errors in quadrature. For comparison, the solid line shows the expected statistical error for 200 fb^{-1} . The vertical line at 145 GeV separates analyses optimized for small [33] and large [32] Higgs masses.

(iii) $H \rightarrow WW \rightarrow \ell^+ \ell^- p_T$

The most challenging WBF channel is $H \rightarrow WW^{(*)}$ decay which does not allow for direct Higgs mass reconstruction and, hence, precludes a simple sideband determination of backgrounds. The important backgrounds [32, 33] involve (virtual) W pairs, namely top decays in $t\bar{t}+jets$ production, and QCD and electroweak $WWjj$ production. QCD and EW $\tau\tau jj$ production are subdominant after cuts, they are known at NLO [38], and they can be determined directly, in phase space regions for jets which are identical to the signal region and with high statistics, by studying e^+e^- or $\mu^+\mu^-$ pairs instead of $\tau^+\tau^-$.

Demands on QCD calculations can be estimated by comparing the effects of systematic background errors on the measurement of the signal rate with statistical errors achievable at the LHC with 200 fb^{-1} of data. Results are shown in Fig. 5 for an assumed 10% error on $\sigma(tt+jets)$, a 50% error on the QCD $WWjj$ rate, and a 30% error on the electroweak $WWjj$ rate. The latter two should be achievable from a LO extrapolation from signal poor to signal rich regions of phase space. A 10% error of $\sigma(tt+jets)$, on the other hand, may require a NLO calculation, in particular of the on-shell $t\bar{t} + 1$ jet cross section which dominates the $t\bar{t}$ background. Off-shell effects have recently been studied at LO [26] and a $\mathcal{O}(20\%)$ increase of the $t\bar{t}$ background was found, which, presumably, is small enough to

permit the inclusion of off-shell effects at LO only. However, a dedicated study is needed to devise optimal techniques for a reliable background determination for $H \rightarrow WW$ searches in WBF, for all major backgrounds.

(iv) Jet veto and Jet Tagging

Background suppression in the WBF channels relies on double forward jet tagging to identify the scattered quark jets of the $qq \rightarrow qqH$ signal and it employs a veto of relatively soft central jets (typically of $p_T > 20$ GeV) to exploit the different gluon radiation patterns and QCD scales of t -channel color singlet versus color octet exchange. Transverse momenta of these tagging or veto jets are relatively small for fixed order perturbative calculations of hard processes at the LHC. Thus, dedicated studies will be needed to assess the applicability of NLO QCD for the modeling of tagging jets in WBF and for the efficiency of a central jet veto in the Higgs signal. First such studies have been performed in the past at LO, for Wjj or Zjj events [40]. While NLO Monte Carlos for QCD Vjj production are now available [38, 41], the corresponding NLO determination of electroweak Vjj cross sections would be highly desirable. This would allow a comparison of calculated and measured veto efficiencies in a WBF process. These efficiencies must be known at the few percent level for the signal in order to extract Higgs couplings without loss of precision.

At present, the veto efficiencies for signal and background processes are the most uncertain aspect of WBF Higgs production at the LHC. Any improvement in their understanding, from QCD calculations, from improved Monte Carlo tools, or from hadron collider data would be very valuable.

4 $t\bar{t}\phi$ production

SM Higgs boson production in association with $t\bar{t}$ pairs plays a significant role at the LHC for Higgs masses below about 130 GeV, since this production mechanism makes the observation of $H \rightarrow b\bar{b}$ possible [7, 18, 42, 43]. The decay $H \rightarrow \gamma\gamma$ is potentially visible in this channel at high integrated luminosity. For Higgs masses above about 130 GeV, the decay $H \rightarrow W^+W^-$ can be observed [44]. $t\bar{t}H$ production could conceivably be used to determine the top Yukawa coupling directly from the cross section, but this requires either assumptions about the branching ratio for $H \rightarrow b\bar{b}$, which are not justified in extensions of the SM, or observability of decay to either $\gamma\gamma$ or W^+W^- . Recently, the NLO QCD corrections have become available. They decrease the cross section at the Tevatron by about 20–30% [45, 46], while they increase the signal rate at the LHC by about 20–40% [45]. The scale dependence of the production cross section is significantly reduced, to a level of about 15%, which can be considered as an estimate of the theoretical uncertainty. Thus, the signal rate is under proper theoretical control now. In the MSSM, $t\bar{t}h$ production with $h \rightarrow \gamma\gamma, b\bar{b}$ is important at the LHC in the decoupling regime, where the light scalar h behaves as the SM Higgs boson [7, 18, 42, 43]. Thus, the SM results can also be used for $t\bar{t}h$ production in this regime.

(i) $t\bar{t}\phi \rightarrow t\bar{t}b\bar{b}$

The major backgrounds to the $\phi \rightarrow b\bar{b}$ signal in associated $t\bar{t}\phi$ production come from $t\bar{t}jj$

and $t\bar{t}b\bar{b}$ production, where in the first case the jets may be misidentified as b jets. A full LO calculation is available for these backgrounds and will be included in the conventional Monte Carlo programs. However, an analysis of the theoretical uncertainties is still missing. A first step can be made by studying the scale dependence at LO in order to investigate the effects on the total normalization and the event shapes. But for a more sophisticated picture a full NLO calculation is highly desirable. A second question is whether these backgrounds can be measured in the experiments off the Higgs resonance and extrapolated to the signal region.

(ii) $t\bar{t}\phi \rightarrow t\bar{t}\gamma\gamma$

The $t\bar{t}\gamma\gamma$ final states develop a narrow resonance in the invariant $\gamma\gamma$ mass distribution, which enables a measurement of the $t\bar{t}\gamma\gamma$ background directly from the sidebands.

(iii) $t\bar{t}\phi \rightarrow t\bar{t}W^+W^-$

This channel does not allow reconstruction of the Higgs. Instead, it relies on a counting experiment of multiplepton final states where the background is of approximately the same size as the signal. The principal backgrounds are $t\bar{t}Wjj$ and $t\bar{t}\ell^+\ell^-(jj)$, with minor backgrounds of $t\bar{t}W^+W^-$ and $t\bar{t}t\bar{t}$. For the 3ℓ channel, the largest background is $t\bar{t}\ell^+\ell^-$ where one lepton is lost. It is possible that this rate could be measured directly for the lepton pair at the Z pole and the result extrapolated to the signal region of phase space. However, for $t\bar{t}Vjj$ backgrounds the QCD uncertainties become large and unknown, due to the presence of two additional soft jets in the event. Further investigation of these backgrounds is essential, and will probably require comparison with data, which is not expected to be trivial.

5 $b\bar{b}\phi$ production

In supersymmetric theories $b\bar{b}\phi$ production becomes the dominant Higgs boson production mechanism for large values of $\tan\beta$ [10], where the bottom Yukawa coupling is strongly enhanced. In contrast to $t\bar{t}\phi$ production, however, this process develops potentially large logarithms, $\log m_\phi^2/m_b^2$, in the high-energy limit due to the smallness of the bottom quark mass, which are related to the development of b densities in the initial state. They can be resummed by evolving the b densities according to the Altarelli–Parisi equations and introducing them in the production process [47]. The introduction of conventional b densities requires an approximation of the kinematics of the hard process, i.e. the initial b quarks are assumed to be massless, have negligible transverse momentum and travel predominantly in forward and backward direction. These approximations can be tested in the full $gg \rightarrow b\bar{b}\phi$ process. At the Tevatron it turns out that they are not valid so that the effective cross section for $b\bar{b} \rightarrow \phi$ has to be considered as an overestimate of the resummed result. An improvement of this resummation requires an approach which describes the kinematics of the hard process in a better way. Moreover, since the experimental analyses require 3 or 4 b tags [6, 7], the spectator b quarks need to have a sizeable transverse momentum of at least 15–20 GeV. Thus a resummation of a different type of potentially arising logarithms, namely $\log m_\phi^2/(m_b^2 + p_{tmin}^2)$ is necessary. This can be achieved by

the introduction of e.g. unintegrated parton densities [48] or an extension of the available resummation techniques.

As a first step, however, we have to investigate if the energy of the Tevatron and LHC is sufficiently large to develop the factorization of bottom densities. This factorization requires that the transverse momentum distribution of the (anti)bottom quark scales like $d\sigma/dp_{Tb} \propto p_{Tb}/(m_b^2 + p_{Tb}^2)$ for transverse momenta up to the factorization scale of the (anti)bottom density. The transverse momentum distributions at the LHC are shown in

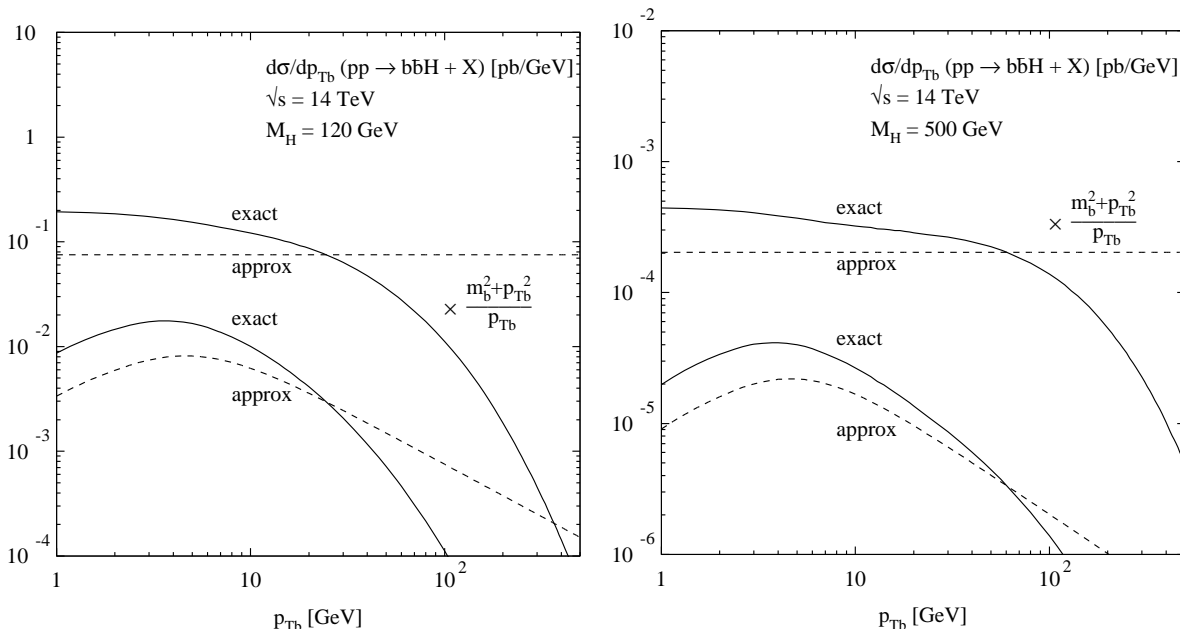


Figure 6: *Transverse momentum distributions of the bottom quark in $b\bar{b}H$ production for two different Higgs masses at the LHC. We have adopted CTEQ5M1 parton densities and a bottom mass of $m_b = 4.62$ GeV. The solid lines show the full LO result from $q\bar{q}, gg \rightarrow b\bar{b}H$ and the dashed lines the factorized collinear part, which is absorbed in the bottom parton density. The upper curves are divided by the factor $p_{Tb}/(m_b^2 + p_{Tb}^2)$ of the asymptotic behavior, which is required by factorizing bottom densities.*

Fig. 6, for two different Higgs masses. The solid curves show the full distributions of the $q\bar{q}, gg \rightarrow b\bar{b}\phi$ processes, while the dashed lines exhibit the factorized collinear part, which is absorbed in the bottom density. For a proper factorization, these pairs of curves have to coincide approximately up to transverse momenta of the order of the factorization scale, which is usually chosen to be $\mu_F = \mathcal{O}(m_H)$. It is clearly visible that there are sizeable differences between the full result and the factorized part, which originate from sizeable bottom mass and phase space effects, that are not accounted for by an active bottom parton density. Moreover, the full result falls quickly below the approximate factorized part for transverse momenta of the order of $m_H/10$, which is much smaller than the usual factorization scale used for the bottom densities. We conclude from these plots that $b\bar{b}\phi$ production at the LHC develops sizeable bottom mass effects, so that the use of bottom densities in the process $b\bar{b} \rightarrow \phi$ may lead to an overestimate of the correct theoretical result due to too crude approximations in the kinematics of the hard process. The full NLO calculation of the $gg \rightarrow b\bar{b}\phi$ will yield much more insight into this problem, since

the large logarithms related to the evolution of bottom densities have to appear in the NLO corrections, if the picture of active bottom quarks in the proton is correct.

6 ZH, WH production

Higgsstrahlung in $q\bar{q} \rightarrow WH, ZH$ plays a crucial role for the Higgs search at the Tevatron, while it is only marginal at the LHC. At the Tevatron it provides the relevant production mechanism for Higgs masses below about 130 GeV, where $H \rightarrow b\bar{b}$ decays are dominant [6]. The NLO QCD corrections have been analyzed in the past. They are identical to the QCD corrections to the Drell–Yan processes $q\bar{q} \rightarrow W, Z$, if the LO matrix elements are replaced accordingly. QCD corrections increase the production cross sections by about 30–40% [49, 29].

The most important backgrounds at the Tevatron are Wjj and in particular $Wb\bar{b}$ production. Both are known at NLO and are contained in a NLO Monte Carlo program [41]. The same applies also to the Zjj and in particular $Zb\bar{b}$ backgrounds [27, 38]. In addition, the $t\bar{t}$ background is relevant.

7 Conclusions

Considerable progress has been made recently in improving QCD calculations for Higgs signal and background cross sections at hadron colliders. Noteworthy examples are the NNLO corrections to the gluon fusion cross section [14], the QCD Zjj cross section at NLO [38] and the determination of full finite top and W width corrections to $t\bar{t}$ and $t\bar{t}j$ production at LO [26]. These improvements are crucial for precise coupling determinations of the Higgs boson.

Much additional work is needed to match the statistical power of the LHC. Largely, QCD systematic errors for coupling measurements have not been analyzed yet. Additional NLO tools need to be provided as well, and these include NLO corrections to $t\bar{t}$ production with finite width effects and $t\bar{t}j$ production at zero top width. A better understanding of central jet veto efficiencies is crucial for the study of WBF channels. These are just a few examples where theoretical work is needed. Many more have been highlighted in this review. Higgs physics at the LHC remains a very rich field for phenomenology.

Acknowledgments.

We would like to thank the organizers of the Les Houches workshop for their invitation, warm hospitality and financial support. The work of M.S. has been supported in part by the Swiss Bundesamt für Bildung und Wissenschaft and by the European Union under contract HPRN-CT-2000-00149. The work of D.Z. was partially supported by WARF and under DOE grant No. DE-FG02-95ER40896. Fermilab is operated by URA under DOE contract No. DE-AC02-76CH03000.

References

- [1] P. W. Higgs, Phys. Lett. **12** (1964) 132 and Phys. Rev. **145** (1966) 1156;
F. Englert and R. Brout, Phys. Rev. Lett. **13** (1964) 321;
G. S. Guralnik, C. R. Hagen and T. W. Kibble, Phys. Rev. Lett. **13** (1964) 585.
- [2] For reviews on the Higgs sector in the Standard Model and in its supersymmetric extensions, see J.F. Gunion, H.E. Haber, G.L. Kane and S. Dawson, *The Higgs Hunter's Guide* (Addison–Wesley, Reading, Mass., 1990).
- [3] LEP Higgs Working Group for Higgs boson searches, Proceedings International Europhysics Conference on High Energy Physics (HEP 2001), Budapest, Hungary, 12-18 Jul 2001, hep-ex/0107029 and hep-ex/0107030.
- [4] See e.g. T. Hambye and K. Riessellmann, Phys. Rev. **D55** (1997) 7255.
- [5] M. Carena, M. Quiros and C.E.M. Wagner, Nucl. Phys. **B461** (1996) 407; H.E. Haber, R. Hempfling and A.H. Hoang, Z. Phys. **C75** (1997) 539; S. Heinemeyer, W. Hollik and G. Weiglein, Phys. Rev. **D58** (1998) 091701; R.–J. Zhang, Phys. Lett. **B447** (1999) 89; J. Espinosa and R.–J. Zhang, Nucl. Phys. **B586** (2000) 3; A. Brignole, G. Degrandi, P. Slavich and F. Zwirner, hep-ph/0112177.
- [6] M. Carena et al., Proceedings ‘Physics at Run II: Workshop on Supersymmetry/Higgs’, Batavia, IL, 19-21 Nov 1998, hep-ph/0010338.
- [7] ATLAS Collaboration, Technical Design Report, CERN–LHCC 99–14 (May 1999); CMS Collaboration, Technical Proposal, CERN–LHCC 94–38 (Dec. 1994).
- [8] D. Zeppenfeld, R. Kinnunen, A. Nikitenko and E. Richter-Was, Phys. Rev. **D62** (2000) 013009.
- [9] A. Bialas and P. V. Landshoff, Phys. Lett. **B256** (1991) 540; J.-R. Cudell and O.F. Hernandez, Nucl. Phys. **B471** (1996) 471; V. A. Khoze, A. D. Martin and M. G. Ryskin, hep-ph/0111078 and references therein.
- [10] M. Spira, Fortschr. Phys. **46** (1998) 203.
- [11] S. Dawson, A. Djouadi and M. Spira, Phys. Rev. Lett. **77** (1996) 16.
- [12] A. Djouadi, M. Spira and P.M. Zerwas, Phys. Lett. **B264** (1991) 440; S. Dawson, Nucl. Phys. **B359** (1991) 283; D. Graudenz, M. Spira and P.M. Zerwas, Phys. Rev. Lett. **70** (1993) 1372; S. Dawson and R.P. Kauffman, Phys. Rev. **D49** (1994) 2298; M. Spira, A. Djouadi, D. Graudenz and P.M. Zerwas, Phys. Lett. **B318** (1993) 347, Nucl. Phys. **B453** (1995) 17.
- [13] R.V. Harlander, Phys. Lett. **B492** (2000) 74.
- [14] R. V. Harlander and W. B. Kilgore, hep-ph/0201206.
- [15] M. Krämer, E. Laenen and M. Spira, Nucl. Phys. **B511** (1998) 523.

- [16] S. Catani, D. de Florian and M. Grazzini, JHEP **0105** (2001) 025; R.V. Harlander and W.B. Kilgore, Phys. Rev. **D64** (2001) 013015.
- [17] S. Catani, D. de Florian, M. Grazzini and P. Nason, to appear in the proceedings of the 2001 Les Houches workshop on “Physics at TeV Colliders”.
- [18] V. Drollinger, T. Muller and D. Denegri, hep-ph/0111312.
- [19] T. Binoth, J.P. Guillet, E. Pilon and M. Werlen, Eur. Phys. J. **C16** (2000) 311.
- [20] Z. Bern, A. De Freitas and L.J. Dixon, JHEP **09** (2001) 037.
- [21] S. Catani, D. de Florian and M. Grazzini, JHEP **0201** (2002) 015.
- [22] S. Frixione, P. Nason and G. Ridolfi, Nucl. Phys. **B383** (1992) 3; S. Frixione, Nucl. Phys. **B410** (1993) 280; U. Baur, T. Han and J. Ohnemus, Phys. Rev. **D48** (1993) 5140, Phys. Rev. **D51** (1995) 3381, Phys. Rev. **D48** (1996) 1098, Phys. Rev. **D57** (1998) 2823.
- [23] L.J. Dixon, Z. Kunszt and A. Signer, Phys. Rev. **D60** (1999) 114037.
- [24] T.G. Rizzo, Phys. Rev. **D22** (1980) 389; W.-Y. Keung and W.J. Marciano, Phys. Rev. **D30** (1984) 248; R.N. Cahn, Rep. Prog. Phys. **52** (1989) 389.
- [25] M. Dittmar and H. Dreiner, Phys. Rev. **D55** (1997) 167.
- [26] N. Kauer and D. Zeppenfeld, Phys. Rev. **D65** (2002) 014021.
- [27] R.K. Ellis and S. Veseli, Phys. Rev. **D60** (1999) 011501 and Nucl. Phys. **B511** (1998) 649; J.M. Campbell and R.K. Ellis, Phys. Rev. **D62** (2000) 114012.
- [28] T. Han, G. Valencia and S. Willenbrock, Phys. Rev. Lett. **69** (1992) 3274.
- [29] A. Djouadi and M. Spira, Phys. Rev. **D62** (2000) 014004.
- [30] D. Rainwater and D. Zeppenfeld, JHEP **9712** (1997) 005.
- [31] D. Rainwater, D. Zeppenfeld and K. Hagiwara, Phys. Rev. **D59** (1999) 014037; T. Plehn, D. Rainwater and D. Zeppenfeld, Phys. Rev. **D61** (2000) 093005.
- [32] D. Rainwater and D. Zeppenfeld, Phys. Rev. **D60** (1999) 113004, (E) *ibid.* **D61** (1999) 099901.
- [33] N. Kauer, T. Plehn, D. Rainwater and D. Zeppenfeld, Phys. Lett. **B503** (2001) 113.
- [34] T. Plehn, D. Rainwater and D. Zeppenfeld, Phys. Lett. **B454** (1999) 297.
- [35] V. Del Duca, W. Kilgore, C. Oleari, C. Schmidt and D. Zeppenfeld, Nucl. Phys. **B616** (2001) 367.

- [36] G. Azuelos et al., *Search for the Standard Model Higgs Boson using Vector Boson Fusion at the LHC*, in D. Cavalli et al., “The Higgs working group: Summary report” for Les Houches 2001, arXiv:hep-ph/0203056.
- [37] S. Dawson, R.P. Kauffman, Phys. Rev. Lett. **68** (1992) 2273; R.P. Kauffman, S.V. Desai, D. Risal, Phys. Rev. **D55** (1997) 4005, (E) *ibid.* **D58** (1998) 119901, Phys. Rev. **D59** (1999) 057504.
- [38] J. Campbell and R. K. Ellis, hep-ph/0202176.
- [39] S. Jadach, J.H. Kühn and Z. Was, Comput. Phys. Commun. **64** (1990) 275; S. Jadach, Z. Was, R. Decker and J.H. Kühn, Comput. Phys. Commun. **76** (1993) 361.
- [40] H. Chehime and D. Zeppenfeld, Phys. Rev. **D47** (1993) 3898; D. Rainwater, R. Szalapski and D. Zeppenfeld, Phys. Rev. **D54** (1996) 6680.
- [41] J. Campbell and R.K. Ellis, <http://theory.fnal.gov/people/ellis/Programs/mcfm.html>
- [42] M. Sapinski and D. Cavalli, Acta Phys. Polon. **B32** (2001) 1317; E. Richter-Was and M. Sapinski, Acta Phys. Polon. **B30** (1999) 1001.
- [43] D. Green, K. Maeshima, R. Vidal, W. Wu and S. Kunori, FERMILAB-FN-0705.
- [44] F. Maltoni, D. Rainwater and S. Willenbrock, hep-ph/0202205.
- [45] W. Beenakker, S. Dittmaier, M. Krämer, B. Plümper, M. Spira and P.M. Zerwas, Phys. Rev. Lett. **87** (2001) 201805.
- [46] L. Reina and S. Dawson, Phys. Rev. Lett. **87** (2001) 201804.
- [47] D.A. Dicus and S. Willenbrock, Phys. Rev. **D39** (1989) 751.
- [48] J. Kwiecinski, A.D. Martin and A.M. Stasto, Phys. Rev. **D56** (1997) 3991; M.A. Kimber, A.D. Martin and M.G. Ryskin, Eur. Phys. J. **C12** (2000) 655.
- [49] T. Han and S. Willenbrock, Phys. Lett. **B273** (1991) 167.